


Observation of J/ψ decays to $e^+e^-e^+e^-$ and $e^+e^-\mu^+\mu^-$

M. Ablikim *et al.**
(BESIII Collaboration)

 (Received 30 November 2021; accepted 1 February 2024; published 18 March 2024)

Using a data sample of 4.481×10^8 $\psi(3686)$ events collected with the BESIII detector, we report the first observation of the four-lepton-decays $J/\psi \rightarrow e^+e^-e^+e^-$ and $J/\psi \rightarrow e^+e^-\mu^+\mu^-$ utilizing the process $\psi(3686) \rightarrow \pi^+\pi^-J/\psi$. The branching fractions are determined to be $[5.48 \pm 0.31(\text{stat}) \pm 0.45(\text{syst})] \times 10^{-5}$ and $[3.53 \pm 0.22(\text{stat}) \pm 0.13(\text{syst})] \times 10^{-5}$, respectively. The results are consistent with theoretical predictions. No significant signal is observed for $J/\psi \rightarrow \mu^+\mu^-\mu^+\mu^-$, and an upper limit on the branching fraction is set at 1.6×10^{-6} at the 90% confidence level. A CP asymmetry observable is constructed for the first two channels, which is measured to be $(-0.012 \pm 0.054 \pm 0.010)$ and $(0.062 \pm 0.059 \pm 0.006)$, respectively. No evidence for CP violation is observed in this process.

DOI: 10.1103/PhysRevD.109.052006

I. INTRODUCTION

Quantum electrodynamics (QED), which describes the electromagnetic interactions, is one of the most accurate theories in the Standard Model (SM). Pure leptonic processes are the golden channels to test QED predictions, compared to semileptonic decays, where the calculations have large uncertainties because of nonperturbative effects. However, there are very few pure leptonic decays without neutrinos in the final states in the τ -charm energy region. $J/\psi \rightarrow \ell^+\ell^-$, where ℓ may be either e or μ , are two such precisely measured channels, and their measured branching fractions (BFs) are consistent with QED calculations [1]. Other purely leptonic decays, which have never been studied experimentally, are $J/\psi \rightarrow \ell_1^+\ell_1^-\ell_2^+\ell_2^-$, where $\ell_1 = \ell_2 = e$, $\ell_1 = \ell_2 = \mu$ or $\ell_1 = e$ and $\ell_2 = \mu$. For the first two cases, there is no special order for the four leptons.

Recently, the branching fractions of $J/\psi \rightarrow \ell_1^+\ell_1^-\ell_2^+\ell_2^-$ decays were calculated at the lowest order in nonrelativistic quantum chromodynamics (NRQCD) factorization in the SM [2]. The smaller lepton mass would generate stronger collinear enhancement according to a recent explicit leading-order QED analysis [2]. Therefore, the predicted branching fraction of $J/\psi \rightarrow e^+e^-e^+e^-$ is $(5.288 \pm 0.028) \times 10^{-5}$, significantly greater than that of $J/\psi \rightarrow e^+e^-\mu^+\mu^-$ ($(3.763 \pm 0.020) \times 10^{-5}$) and two orders of magnitude greater than that of $J/\psi \rightarrow \mu^+\mu^-\mu^+\mu^-$ [$(0.0974 \pm 0.0005) \times 10^{-5}$].

*Full author list given at the end of the article.

Published by the American Physical Society under the terms of the [Creative Commons Attribution 4.0 International license](#). Further distribution of this work must maintain attribution to the author(s) and the published article's title, journal citation, and DOI. Funded by SCOAP³.

Therefore, the ratio $\mathcal{B}_{eeee} : \mathcal{B}_{ee\mu\mu} : \mathcal{B}_{\mu\mu\mu\mu}$ provides a good opportunity to verify the validity of lepton flavor universality (LFU), where \mathcal{B}_{eeee} , $\mathcal{B}_{ee\mu\mu}$ and $\mathcal{B}_{\mu\mu\mu\mu}$ represent the BFs of the $J/\psi \rightarrow e^+e^-e^+e^-$, $J/\psi \rightarrow e^+e^-\mu^+\mu^-$ and $J/\psi \rightarrow \mu^+\mu^-\mu^+\mu^-$ decays, respectively.

In addition, to date, all effects observed so far of charge-parity (CP) violation in particle decays cannot explain the observed matter-antimatter asymmetry in the Universe, motivating further searches for new sources of CP violation. Any new CP violation mechanism is usually constrained by the neutron electric dipole moment (nEDM) [3–5]. Recently, Sanchez-Puertas [6] proposed a new test for CP violation in the electromagnetic decay $\eta \rightarrow \mu^+\mu^-e^+e^-$, in which the sources of CP violation are derived from dimension-six terms in the Standard Model effective field theory [7]. This purely leptonic decay avoids the strong constraints from the nEDM and could be studied at the proposed η facility experiment REDTOP [8]. Similarly, a test can be performed in leptonic decays of $J/\psi \rightarrow \ell_1^+\ell_1^-\ell_2^+\ell_2^-$ at BESIII, especially for the decay of $J/\psi \rightarrow e^+e^-\mu^+\mu^-$.

Using the world's largest $\psi(3686)$ data samples collected with the BESIII detector [9], we search for the decays $J/\psi \rightarrow \ell_1^+\ell_1^-\ell_2^+\ell_2^-$ with J/ψ events from $\psi(3686) \rightarrow \pi^+\pi^-J/\psi$ [10]. Because of the enormous QED background from the two photon process, $e^+e^- \rightarrow \gamma^*\gamma^* \rightarrow \ell_1^+\ell_1^-\ell_2^+\ell_2^-$, this analysis is performed using J/ψ events from $\psi(3686)$ decays instead of those from the larger J/ψ data set. Although the total number of J/ψ events from $\psi(3686)$ decays is one order of magnitude smaller, the QED background can be suppressed to a negligible level by the requirement that the $\pi^+\pi^-$ recoil mass is near the J/ψ mass.

This paper reports the first measurement of the branching fractions of the decays $J/\psi \rightarrow \ell_1^+\ell_1^-\ell_2^+\ell_2^-$, which can be compared with theoretical calculations. The asymmetries

of a CP observable constructed by a T-odd triple-product [11–15] are presented for the first two channels ($J/\psi \rightarrow e^+e^-e^+e^-$ and $J/\psi \rightarrow e^+e^-\mu^+\mu^-$).

II. BESIII DETECTOR AND DATASET

Details about the design and performance of the BESIII detector are given in Refs. [9,16,17]. Monte Carlo (MC) simulated data samples produced with a Geant4-based [18] software package, which includes the geometric description of the BESIII detector and the detector response, are used to determine the detection efficiencies and to estimate backgrounds. The simulation includes the beam energy spread and initial state radiation in the e^+e^- annihilations modeled with the generator KKMC [19,20]. The data sample consists of $(448.1 \pm 2.9) \times 10^6$ $\psi(3686)$ events [21] collected with the BESIII detector. Comparable amounts of inclusive MC simulated events are used to study the backgrounds from $\psi(3686)$ decays. The production of the $\psi(3686)$ resonance is simulated by the MC event generator KKMC [19,20]. The known decay modes are generated by EvtGen [22,23] with branching fractions taken from the Particle Data Group (PDG) [24], and the remaining unknown decays are generated with the LUNDCHARM model [25,26]. For the signal MC, the $\psi(3686) \rightarrow \pi^+\pi^-J/\psi$ channel is generated by JPIPI [22,23], and the simulation of the $J/\psi \rightarrow \ell_1^+\ell_1^-\ell_2^+\ell_2^-$ decay includes the polarization of the J/ψ and the angular distributions of the final states. Since the $\pi^+\pi^-$ system is dominated by the S-wave [10,27], the produced J/ψ fully inherits the state of the $\psi(3686)$ polarization.

III. EVENT SELECTION

Charged particle tracks in the polar angle range $|\cos\theta| < 0.93$ are reconstructed from hits in the main drift chamber (MDC). Tracks with their point of closest approach to the beam line within ± 10 cm of the interaction point (IP) in the beam direction, and within 1 cm in the plane perpendicular to the beam, are selected. At least six charged tracks fulfilling these criteria are required. The time-of-flight and specific energy loss (dE/dx) information are used to calculate particle identification (PID) probabilities (prob) for the electron, pion, muon and kaon hypotheses. A track is considered to be an electron if it satisfies $\text{prob}(e) > \text{prob}(\pi)$ and $\text{prob}(e) > \text{prob}(K)$. For the two channels with muons in the final states, muon candidates must satisfy $\text{prob}(\mu) > \text{prob}(e)$ and $\text{prob}(\mu) > \text{prob}(K)$, and the deposited energy in the calorimeter (E_{EMC}) for the muon candidate must be in the range of [0.1, 0.3] GeV. Any track not identified as an electron or muon is assigned as a pion.

To identify $\pi^+\pi^-J/\psi$ candidates, two oppositely charged tracks with momentum less than 0.45 GeV/ c are required and are used to calculate the mass recoiling against them, $M_{\pi^+\pi^-}^{\text{rec}}$. Using double Gaussian functions, fits are performed on the $M_{\pi^+\pi^-}^{\text{rec}}$ distributions of data, as shown in Figs. 1(a) and 1(c). The combinations with $M_{\pi^+\pi^-}^{\text{rec}}$ within a

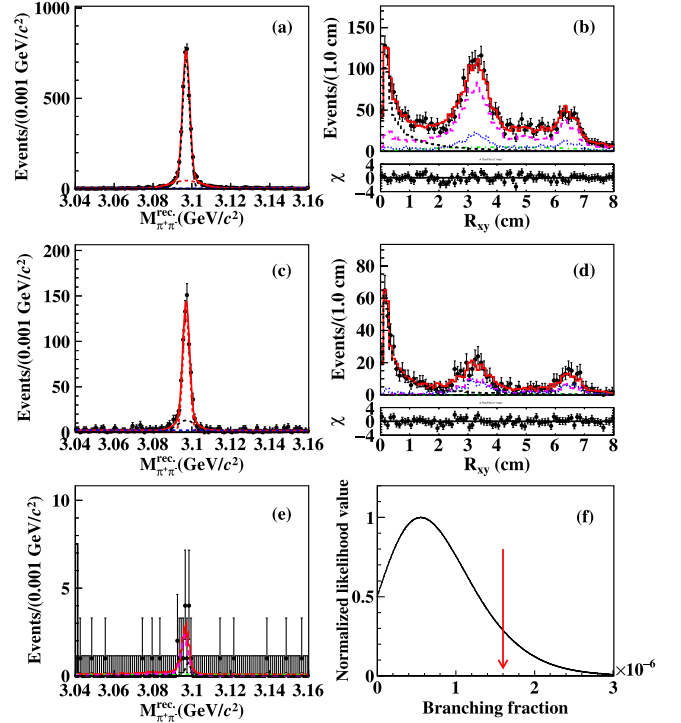


FIG. 1. (a) Fit to the $M_{\pi^+\pi^-}^{\text{rec}}$ distribution of the $\psi(3686)$ data using a double Gaussian function for $J/\psi \rightarrow e^+e^-e^+e^-$ channel. (b) Fit to the R_{xy} distribution of for $J/\psi \rightarrow e^+e^-e^+e^-$ channel. The black error bars represent data, the red solid curve indicates the overall fit, the black dashed line shows the signal, the blue dotted line is the inclusive MC background, the pink dashed line is the $J/\psi \rightarrow \gamma e^+e^-$ background and the green dash-dotted line is the continuum background. (c) Fit to the $M_{\pi^+\pi^-}^{\text{rec}}$ distribution using a double Gaussian function for the $J/\psi \rightarrow e^+e^-\mu^+\mu^-$ channel. (d) Fit to the R_{xy} distribution for the $J/\psi \rightarrow e^+e^-\mu^+\mu^-$ channel. (e) Fit to the $M_{\pi^+\pi^-}^{\text{rec}}$ distribution for the $J/\psi \rightarrow \mu^+\mu^-\mu^+\mu^-$ channel. (f) Likelihood distribution versus the branching fraction of the $J/\psi \rightarrow \mu^+\mu^-\mu^+\mu^-$ decay mode. The red arrow indicates the UL at the 90% confidence level.

5σ mass window around the J/ψ peak are retained, where σ is the resolution of the fitted double Gaussian function ($\sigma = 4.0 \pm 0.2$ MeV/ c^2 for the $J/\psi \rightarrow e^+e^-e^+e^-$ channel; $\sigma = 2.8 \pm 0.5$ MeV/ c^2 for the $J/\psi \rightarrow e^+e^-\mu^+\mu^-$ channel). An energy-momentum constraint (4C) kinematic fit is performed on the selected $\psi(3686) \rightarrow \pi^+\pi^-J/\psi$, $J/\psi \rightarrow \ell_1^+\ell_1^-\ell_2^+\ell_2^-$ candidate events. For the channel $J/\psi \rightarrow e^+e^-e^+e^-$, if more than one combination satisfies the 4C fit, the combination with the smallest χ_{4C}^2 is retained. For the last two channels, the combination with $M_{\pi^+\pi^-}^{\text{rec}}$ closest to the nominal J/ψ mass is selected. The χ_{4C}^2 values of the candidate events are required to be less than 200.

To remove the $J/\psi \rightarrow e^+e^-\pi^+\pi^-$ and $J/\psi \rightarrow \pi^+\pi^-\pi^+\pi^-$ backgrounds, additional 4C kinematic fits are performed, and events with $\chi_{4C}^2(J/\psi \rightarrow e^+e^-\mu^+\mu^-) < \chi_{4C}^2(J/\psi \rightarrow e^+e^-\pi^+\pi^-)$ and $\chi_{4C}^2(J/\psi \rightarrow \mu^+\mu^-\mu^+\mu^-) < \chi_{4C}^2(J/\psi \rightarrow \pi^+\pi^-\pi^+\pi^-)$ are retained for the last two

channels, respectively. After the above selection criteria are applied, about 72% $J/\psi \rightarrow e^+e^-\pi^+\pi^-$ backgrounds and 85% $J/\psi \rightarrow \pi^+\pi^-\pi^+\pi^-$ backgrounds are eliminated. To remove possible contamination from the backgrounds with six charged tracks in the final state, four of which are from J/ψ decays, such as $J/\psi \rightarrow 2(\pi^+\pi^-)$, $J/\psi \rightarrow 2(\pi K)$, and $J/\psi \rightarrow 2(K^+K^-)$, etc., we apply further muon PID requirements for the $J/\psi \rightarrow \mu^+\mu^-\mu^+\mu^-$ decay channel. The selection criteria of the depth in the muon counters of the muon candidate are the same as Ref. [28].

Possible background contributions are studied with data taken at $\sqrt{s} = 3.773$ GeV [29] and the $\psi(3686)$ inclusive MC sample. The former indicates that the QED background is negligible. Examination of the latter with an event topology analysis tool, TopoAna [30], shows that the dominant backgrounds are from the channels $J/\psi \rightarrow \gamma e^+e^-$ and $J/\psi \rightarrow \gamma_{\text{FSR}}e^+e^-$ for the $J/\psi \rightarrow e^+e^-e^+e^-$ decay, $J/\psi \rightarrow \gamma\mu^+\mu^-$ and $J/\psi \rightarrow \gamma_{\text{FSR}}\mu^+\mu^-$ for $J/\psi \rightarrow e^+e^-\mu^+\mu^-$ and $J/\psi \rightarrow \mu^+\mu^-\mu^+\mu^-$ decay modes, where γ_{FSR} is a photon from the final-state radiation which converts to an e^+e^- pair in the detector material. For the $J/\psi \rightarrow \mu^+\mu^-\mu^+\mu^-$ channel, two background events from $J/\psi \rightarrow \pi^+\pi^-\pi^+\pi^-$ in the inclusive MC sample survive the above selection criteria and are considered as peaking background.

A photon-conversion finder [31] is used to reconstruct the photon conversion point. The distance from the IP to the reconstructed conversion point of the lower momentum e^+e^- pair, R_{xy} , is used to separate the signal events from the photon conversion background events. For the $J/\psi \rightarrow e^+e^-e^+e^-$ and $J/\psi \rightarrow e^+e^-\mu^+\mu^-$ signal events, the R_{xy} distribution accumulates around 0 cm, because the e^+e^- pair comes directly from the J/ψ decay. For the photon conversion background, which is usually associated with the lower momentum e^+e^- pair, most of the photon conversions occur in the beam pipe and inner wall of the MDC, and the R_{xy} distribution accumulates beyond 2 cm. However, there can be some contamination under the peak at $R_{xy} = 0$ from events where another e^+e^- pair occurs from photon conversion. Usually the conversion pairs in these events have similar momentum with the lower momentum pair. In order to remove this background, the differences of the momenta between the two electrons and the two positrons in the final state are required to be greater than 1.0 GeV/c, i.e. $\Delta p = (p_{e_h^\pm} - p_{e_l^\pm}) > 1.0$ GeV/c (e_l^\pm : e^\pm with lower momentum, e_h^\pm : e^\pm with higher momentum).

IV. BRANCHING-FRACTION MEASUREMENT

In order to determine the signal yields, unbinned maximum likelihood fits are performed on the R_{xy} distributions for the first two decay modes and to the $\pi^+\pi^-$ recoil mass ($M_{\pi^+\pi^-}^{\text{rec}}$) spectrum for the $J/\psi \rightarrow \mu^+\mu^-\mu^+\mu^-$ channel, as shown in Figs. 1(b), 1(d) and 1(e), respectively. In the fits to the R_{xy} distributions for the first two channels,

the signal is described by signal MC shape, while the background is described by a combination of the inclusive MC, the exclusive $J/\psi \rightarrow \gamma e^+e^-$ ($J/\psi \rightarrow \gamma\mu^+\mu^-$) MC, and a second-order polynomial function. For the $J/\psi \rightarrow \mu^+\mu^-\mu^+\mu^-$ channel, the signal is described by a MC-simulated shape convolved with a Gaussian function, while the background is described by a combination of the $J/\psi \rightarrow \pi^+\pi^-\pi^+\pi^-$ MC shape and a first-order polynomial function. The number of events of the peaking background from $J/\psi \rightarrow \pi^+\pi^-\pi^+\pi^-$ is fixed to the value estimated using the world average branching fraction [24]. The fitted signal yields, detection efficiencies and measured branching fractions are listed in Table I. The measured branching fractions are determined by

$$\mathcal{B}(J/\psi \rightarrow \ell_1^+\ell_1^-\ell_2^+\ell_2^-) = \frac{N_{\text{sig}}}{N_{\psi(3686)} \cdot \epsilon \cdot \mathcal{B}(\psi(3686))}, \quad (1)$$

where N_{sig} is the number of observed signal events, $N_{\psi(3686)}$ is the number of $\psi(3686)$ events [21], and ϵ is the detection efficiency determined by MC simulation. The branching fraction $\mathcal{B}(\psi(3686)) \equiv \mathcal{B}(\psi(3686) \rightarrow \pi^+\pi^- J/\psi)$ is taken from the PDG [24]. To obtain a more accurate of detecting the decay of $J/\psi \rightarrow e^+e^-e^+e^-$, the events of the signal MC sample are weighted according to the e_l^+ momentum versus e_l^- momentum distribution in data. The weight factors are the $\epsilon_{\text{data}}^i/\epsilon_{\text{MC}}^i$ ratios which are obtained in different momentum bins, where ϵ_{data}^i and ϵ_{MC}^i are the efficiencies of $e^+e^-e^+e^-$ candidates in the i th bin from data and MC simulation, respectively. The resultant detection efficiency is $(8.22 \pm 0.02)\%$.

V. SYSTEMATIC UNCERTAINTIES

The following sources of systematic uncertainty for the branching fraction measurement are considered; tracking efficiency, PID efficiency, total number of $\psi(3686)$ events, branching fraction of $\psi(3686) \rightarrow \pi^+\pi^- J/\psi$, kinematic fit, $\pi^+\pi^-$ recoil mass window, fit range, signal PDF shape, background PDF shape, and the Δp cut.

To study the systematic uncertainties related to the tracking and PID efficiencies of electrons and positrons, control samples of radiative Bhabha events are selected, i.e. $e^+e^- \rightarrow \gamma e^+e^-$, at the $\psi(3686)$ energy for both the experimental data and MC simulation. The differences between the data and MC simulation in different momentum and polar angle regions are obtained from the control samples. The systematic uncertainties are calculated according to the momentum and polar angle distributions in the signal MC sample. They are assigned as 1.1% and 0.3% from tracking efficiencies, 2.0% and 1.7% from PID efficiencies of the first two channels, respectively.

The systematic uncertainties from the tracking and PID efficiencies of muons are estimated through a control sample of $e^+e^- \rightarrow (\gamma)\mu^+\mu^-$ [28]. The uncertainties from the tracking and PID efficiencies of each muon track are

0.1% and 0.8%, respectively. The systematic uncertainties from the pion tracking efficiency are estimated through a control sample of $\psi(3686) \rightarrow \pi^+\pi^-J/\psi$, which gives 1% for each pion track [32]. The systematic uncertainty on the number of $\psi(3686)$ events is 0.6% [21], and the uncertainty of the branching fraction of $\psi(3686) \rightarrow \pi^+\pi^-J/\psi$ is 0.9% [24].

In the 4C kinematic fits, the helix parameters of simulated charged tracks are corrected to reduce the discrepancy between data and MC simulation as described in Ref. [33]. The correction factors are obtained by studying a control sample of $\psi(3686) \rightarrow \pi^+\pi^-J/\psi, J/\psi \rightarrow \ell^+\ell^-$. The MC samples with the corrected track helix parameters are taken as the nominal ones. The differences between detection efficiencies obtained from MC samples with and without the correction are taken as the uncertainties, which are 1.0%, 0.7% and 0.9% for the three channels, respectively.

The systematic uncertainties due to the maximum likelihood fits are studied as follows: For the first two channels, the signal shape is replaced with the signal MC convolved with a Gaussian function, and the uncertainties from the signal shape are evaluated to be 1.7% and 1.2%, respectively. The second-order polynomial function is changed to a third-order one to estimate the uncertainties from the background PDF shape, which are assigned to be 0.8% and 0.1%, respectively. To evaluate the systematic effects from the requirement on the recoil mass of $\pi^+\pi^-$, an alternative shape from the signal MC sample is used. The relative differences in the number of signal events, 0.4% and 0.1%, respectively, are taken as the systematic uncertainties. To estimate the systematic uncertainties from the fit range, the range of R_{xy} is changed from [0.0, 8.0] to [0.0, 9.0], and the changes of the measured branching fractions are taken as the systematic uncertainties, which are evaluated to be 1.0% and 0.1%, respectively. The systematic uncertainty from the selection on Δp is estimated by using a different requirement $[(p_{e_h^\pm} - p_{e_l^\pm}) > 1.10 \text{ GeV}/c]$ on this variable, set to be 3.0%. To obtain reliable signal efficiency, the signal MC sample $J/\psi \rightarrow e^+e^-e^+e^-$ is weighted to match the data. To estimate the associated systematic uncertainty, the weight factors are randomly changed within one standard deviation in each bin one thousand times to re-obtain the signal efficiency. The distribution of the resulting signal efficiency is fit with a Gaussian function, and the

standard deviation of 6.5% is taken as the systematic uncertainty. For the $J/\psi \rightarrow \mu^+\mu^-\mu^+\mu^-$ mode, the $\pi^+\pi^-$ recoil mass window is changed from [3.04, 3.16] GeV/c^2 to [3.06, 3.16] GeV/c^2 , and 0.9% is taken as the systematic uncertainty from this source. The first-order polynomial function is changed to a second-order one to estimate the uncertainty from the background PDF shape, which is assigned to be 0.3%. In estimating the uncertainty from the background events of $J/\psi \rightarrow \pi^+\pi^-\pi^+\pi^-$, the fits are performed twenty thousand times with the number of the background events sampled from a Gaussian distribution based on its statistical error. The distribution of the relative difference on the signal yield is fitted by a Gaussian function, and its width of 0.2% is assigned as the systematic uncertainty from this source. The total systematic uncertainties of the BF measurement are 8.2%, 3.6%, and 4.2% for the three channels, respectively, obtained by adding the above effects quadratically.

VI. DETERMINE THE UPPER LIMIT

As indicated in Fig. 1(e), no significant signal is observed for the $J/\psi \rightarrow \mu^+\mu^-\mu^+\mu^-$ channel, so the branching fraction upper limit (UL) is determined according to Eq. (1) based on a Bayesian method [34]. A series of fits of the $M_{\pi^+\pi^-}^{\text{rec}}$ distribution are carried out fixing the BF at different values, and the resultant curve of likelihood values as a function of the BF is convolved with a Gaussian function to take into account the overall systematic uncertainty, as shown in Fig. 1(f). The UL on the BF is obtained when the integral of the likelihood curve in the positive domain reaches 90% of its total value.

VII. CP ASYMMETRY MEASUREMENT

Following Refs. [11,12], we measure correlations between the final state leptons. In the rest frame of J/ψ , we define $C_T = (\vec{p}_{\ell_a^+} \times \vec{p}_{\ell_a^-}) \cdot \vec{p}_{\ell_b^+}$, where ℓ_a and ℓ_b are final-state leptons; $\ell_a = \ell_b = e$ for $J/\psi \rightarrow e^+e^-e^+e^-$, while $\ell_a = e$ and $\ell_b = \mu$ for $J/\psi \rightarrow e^+e^-\mu^+\mu^-$. In the former case, ℓ_a^+ and ℓ_a^- are taken as the leptons with lower momenta, and ℓ_b^+ those with higher momenta [11,35]. A CP asymmetry observable based on CPT invariance [11,12], \mathcal{A}_T , can be constructed with the number of events of positive and negative C_T values:

TABLE I. Observed signal yields, detection efficiencies, numbers of observed events with $C_T > 0$ and $C_T < 0$, measured branching fraction and \mathcal{A}_T values for different decay modes. The first uncertainty is statistical and the second is systematic.

Decay mode	N_{sig}	$\epsilon(\%)$	This work			\mathcal{A}_T	Theory [2]
			$N(C_T > 0)$	$N(C_T < 0)$	$\mathcal{B}(\times 10^{-5})$		$\mathcal{B}(\times 10^{-5})$
$J/\psi \rightarrow e^+e^-e^+e^-$	700 ± 39	8.22 ± 0.02	355 ± 27	363 ± 28	$5.48 \pm 0.31 \pm 0.45$	$-0.012 \pm 0.054 \pm 0.010$	5.288 ± 0.028
$J/\psi \rightarrow e^+e^-\mu^+\mu^-$	354 ± 22	6.46 ± 0.04	193 ± 15	170 ± 15	$3.53 \pm 0.22 \pm 0.13$	$0.062 \pm 0.059 \pm 0.006$	3.763 ± 0.020
$J/\psi \rightarrow \mu^+\mu^-\mu^+\mu^-$	3.4 ± 4.1	3.96 ± 0.03	< 0.16	...	0.0974 ± 0.0005

$$A_T = \frac{N(C_T > 0) - N(C_T < 0)}{N(C_T > 0) + N(C_T < 0)}. \quad (2)$$

The numbers of events with $C_T > 0$ and $C_T < 0$ are evaluated by a simultaneous fit to the R_{xy} distributions of data using the same fit method as that used in the branching fraction measurements. The parameters of the signal shape are shared in the fits, while the other parameters are free. Taking into account the contributions of the same systematic uncertainties as in the branching fraction measurement, the respective numbers of events and measured asymmetries of the $J/\psi \rightarrow e^+e^-e^+e^-$ and $J/\psi \rightarrow e^+e^-\mu^+\mu^-$ channels are listed in Table I.

VIII. SUMMARY

In summary, based on a data sample of 4.481×10^8 $\psi(3686)$ events collected with the BESIII detector, the decay processes of $J/\psi \rightarrow \ell_1^+\ell_1^-\ell_2^+\ell_2^-$ are investigated. The decay channels of $J/\psi \rightarrow e^+e^-e^+e^-$ and $J/\psi \rightarrow e^+e^-\mu^+\mu^-$ are observed for the first time, and the corresponding branching fractions are measured. The theoretical predictions based on NRQCD [2] are consistent with our measurements of the branching fractions for these two channels. No signal is observed for the $J/\psi \rightarrow \mu^+\mu^-\mu^+\mu^-$ channel, and the UL of the branching fraction is determined. No CP violation is observed. All measured results are summarized in Table I. The ratio $\mathcal{B}_{eeee}/\mathcal{B}_{ee\mu\mu}$ is calculated to be $(1.55 \pm 0.13 \pm 0.14)$, which agrees with theory within 1σ [2]. The UL on the ratio $\mathcal{B}_{\mu\mu\mu\mu}/\mathcal{B}_{eeee}$ is calculated with

$$\frac{\mathcal{B}_{\mu\mu\mu\mu}}{\mathcal{B}_{eeee}} < \frac{N_{\text{UL}}^{4\mu}/\epsilon^{4\mu}}{N^{4e}/\epsilon^{4e}} \frac{1}{(1 - \sigma_{13})}. \quad (3)$$

Here $N_{\text{UL}}^{4\mu}$ is the 90% UL on the number of observed events for $J/\psi \rightarrow \mu^+\mu^-\mu^+\mu^-$ decay, $\epsilon^{4\mu}$ is the MC-determined efficiency for the channel, N^{4e} is the number of events for the $J/\psi \rightarrow e^+e^-e^+e^-$ decay, ϵ^{4e} is the MC-determined efficiency for this channel, $\sigma_{13} = \sqrt{(\sigma_{13}^{\text{stat}})^2 + (\sigma_{13}^{\text{sys}})^2} = 10.9\%$, where $\sigma_{13}^{\text{stat}}$ is the relative statistical error of N^{4e} (5.7%) and σ_{13}^{sys} is the total relative systematic error for $J/\psi \rightarrow e^+e^-e^+e^-$ and $J/\psi \rightarrow \mu^+\mu^-\mu^+\mu^-$ decay channels.

The UL on the ratio $\mathcal{B}_{\mu\mu\mu\mu}/\mathcal{B}_{eeee}$ is determined to be 0.033. Similarly, the UL on the ratio $\mathcal{B}_{\mu\mu\mu\mu}/\mathcal{B}_{ee\mu\mu}$ is determined to be 0.050.

ACKNOWLEDGMENTS

The BESIII Collaboration thanks the staff of BEPCII and the IHEP computing center for their strong support. The authors would like to extend thanks to Professor Xian-Wei Kang for useful discussions and helpful advice. This work is supported in part by National Key Research and Development Program of China under Contracts No. 2023YFA1606704, No. 2020YFA0406300, and No. 2020YFA0406400; National Natural Science Foundation of China (NSFC) under Contracts No. 12375092, No. 11805037, No. 11975118, and No. 12165022; the Natural Science Foundation of Hunan Province under Contracts No. 2020RC3054 and No. 2019JJ30019; the Chinese Academy of Sciences (CAS) Large-Scale Scientific Facility Program; Joint Large-Scale Scientific Facility Funds of the NSFC and CAS under Contracts No. U1832121, No. U1732263, and No. U1832207; CAS Key Research Program of Frontier Sciences under Contract No. QYZDJ-SSW-SLH040; 100 Talents Program of CAS; INPAC and Shanghai Key Laboratory for Particle Physics and Cosmology; Yunnan Fundamental Research Project under Contract No. 202301AT070162; ERC under Contract No. 758462; European Union Horizon 2020 research and innovation programme under Contract No. Marie Skłodowska-Curie Grant agreement No. 894790; German Research Foundation DFG under Contracts No. 443159800, Collaborative Research Center CRC 1044, FOR 2359, GRK 214; Istituto Nazionale di Fisica Nucleare, Italy; Ministry of Development of Turkey under Contract No. DPT2006K-120470; National Science and Technology fund; Olle Engkvist Foundation under Contract No. 200-0605; STFC (United Kingdom); The Knut and Alice Wallenberg Foundation (Sweden) under Contract No. 2016.0157; The Royal Society, UK under Contracts No. DH140054 and No. DH160214; The Swedish Research Council; U.S. Department of Energy under Contracts No. DE-FG02-05ER41374 and No. DE-SC-0012069.

- [1] M. Ablikim *et al.* (BES Collaboration), *Phys. Lett. B* **761**, 98 (2016).
 [2] W. Chen, Y. Jia, Z. Mo, J. Pan, and X. Xiong, *Phys. Rev. D* **104**, 094023 (2021).
 [3] E. M. Purcell and N. F. Ramsey, *Phys. Rev.* **78**, 807 (1950).
 [4] S. Dar, arXiv:hep-ph/0008248.

- [5] J. M. Pendlebury, S. Afach, N. J. Ayres, C. A. Baker, G. Ban, G. Bison, K. Bodek, M. Burghoff, P. Geltenbort, K. Green *et al.*, *Phys. Rev. D* **92**, 092003 (2015).
 [6] P. Sanchez-Puertas, *J. High Energy Phys.* **01** (2019) 031.
 [7] B. Grzadkowski, M. Iskrzynski, M. Misiak, and J. Rosiek, *J. High Energy Phys.* **10** (2010) 085.

- [8] C. Gatto *et al.* (REDTOP Collaboration), *Proc. Sci. ICHEP2016* (2016) 812.
- [9] M. Ablikim *et al.* (BESIII Collaboration), *Nucl. Instrum. Methods Phys. Res., Sect. A* **614**, 345 (2010).
- [10] J. Z. Bai *et al.* (BES Collaboration), *Phys. Rev. D* **62**, 032002 (2000).
- [11] M. Gronau and J. L. Rosner, *Phys. Rev. D* **84**, 096013 (2011).
- [12] I. I. Bigi, X. W. Kang, and H. B. Li, *Chin. Phys. C* **42**, 013101 (2018).
- [13] X. D. Shi, X. W. Kang, I. Bigi, W. P. Wang, and H. P. Peng, *Phys. Rev. D* **100**, 113002 (2019).
- [14] X. W. Kang and H. B. Li, *Phys. Lett. B* **684**, 137 (2010).
- [15] X. W. Kang, H. B. Li, G. R. Lu, and A. Datta, *Int. J. Mod. Phys. A* **26**, 2523 (2011).
- [16] C. H. Yu *et al.*, *Proceedings of IPAC 2016* (2016), <http://ir.ihep.ac.cn/handle/311005/247347>.
- [17] M. Ablikim *et al.* (BESIII Collaboration), *Chin. Phys. C* **44**, 040001 (2020).
- [18] S. Agostinelli *et al.* (GEANT4 Collaboration), *Nucl. Instrum. Methods Phys. Res., Sect. A* **506**, 250 (2003).
- [19] S. Jadach, B. F. L. Ward, and Z. Was, *Comput. Phys. Commun.* **130**, 260 (2000).
- [20] S. Jadach, B. F. L. Ward, and Z. Was, *Phys. Rev. D* **63**, 113009 (2001).
- [21] M. Ablikim *et al.* (BESIII Collaboration), *Chin. Phys. C* **42**, 023001 (2018).
- [22] R. G. Ping, *Chin. Phys. C* **32**, 599 (2008).
- [23] D. J. Lange, *Nucl. Instrum. Methods Phys. Res., Sect. A* **462**, 152 (2001).
- [24] P. A. Zyla *et al.* (Particle Data Group), *Prog. Theor. Exp. Phys.* **2020**, 083C01 (2020).
- [25] J. C. Chen, G. S. Huang, X. R. Qi, D. H. Zhang, and Y. S. Zhu, *Phys. Rev. D* **62**, 034003 (2000).
- [26] R. L. Yang, R. G. Pong, and H. Chen, *Chin. Phys. Lett.* **31**, 061301 (2014).
- [27] M. Ablikim *et al.* (BES Collaboration), *Phys. Lett. B* **645**, 1 (2007).
- [28] M. Ablikim *et al.* (BESIII Collaboration), *Phys. Rev. D* **89**, 051104 (2014).
- [29] M. Ablikim *et al.* (BESIII Collaboration), *Chin. Phys. C* **37**, 123001 (2013).
- [30] X. Zhou, S. Du, G. Li, and C. Shen, *Comput. Phys. Commun.* **258**, 107540 (2021).
- [31] Z. R. Xu and K. L. He, *Chin. Phys. C* **36**, 742 (2012).
- [32] M. Ablikim *et al.* (BESIII Collaboration), *Phys. Rev. D* **83**, 112005 (2011).
- [33] M. Ablikim *et al.* (BESIII Collaboration), *Phys. Rev. D* **87**, 012002 (2013).
- [34] Y. S. Zhu, *Nucl. Instrum. Methods Phys. Res., Sect. A* **578**, 322 (2007).
- [35] R. Aaij *et al.* (LHCb Collaboration), *Nat. Phys.* **13**, 391 (2017).

M. Ablikim,¹ M. N. Achasov,^{10,c} P. Adlarson,⁶⁷ S. Ahmed,¹⁵ M. Albrecht,⁴ R. Aliberti,²⁸ A. Amoroso,^{66a,66c} M. R. An,³² Q. An,^{63,49} X. H. Bai,⁵⁷ Y. Bai,⁴⁸ O. Bakina,²⁹ R. Baldini Ferroli,^{23a} I. Balossino,^{24a} Y. Ban,^{38,k} K. Begzsuren,²⁶ N. Berger,²⁸ M. Bertani,^{23a} D. Bettoni,^{24a} F. Bianchi,^{66a,66c} J. Bloms,⁶⁰ A. Bortone,^{66a,66c} I. Boyko,²⁹ R. A. Briere,⁵ H. Cai,⁶⁸ X. Cai,^{1,49} A. Calcaterra,^{23a} G. F. Cao,^{1,54} N. Cao,^{1,54} S. A. Cetin,^{53a} J. F. Chang,^{1,49} W. L. Chang,^{1,54} G. Chelkov,^{29,b} D. Y. Chen,⁶ G. Chen,¹ H. S. Chen,^{1,54} M. L. Chen,^{1,49} S. J. Chen,³⁵ X. R. Chen,²⁵ Y. B. Chen,^{1,49} Z. J. Chen,^{20,1} W. S. Cheng,^{66c} G. Cibinetto,^{24a} F. Cossio,^{66c} X. F. Cui,³⁶ H. L. Dai,^{1,49} J. P. Dai,⁷² X. C. Dai,^{1,54} A. Dbeyssi,¹⁵ R. E. de Boer,⁴ D. Dedovich,²⁹ Z. Y. Deng,¹ A. Denig,²⁸ I. Denysenko,²⁹ M. Destefanis,^{66a,66c} F. De Mori,^{66a,66c} Y. Ding,³³ C. Dong,³⁶ J. Dong,^{1,49} L. Y. Dong,^{1,54} M. Y. Dong,^{1,49,54} X. Dong,⁶⁸ S. X. Du,⁷¹ Y. L. Fan,⁶⁸ J. Fang,^{1,49} S. S. Fang,^{1,54} Y. Fang,¹ R. Farinelli,^{24a} L. Fava,^{66b,66c} F. Feldbauer,⁴ G. Felici,^{23a} C. Q. Feng,^{63,49} J. H. Feng,⁵⁰ M. Fritsch,⁴ C. D. Fu,¹ Y. Gao,⁶⁴ Y. Gao,^{63,49} Y. Gao,^{38,k} Y. G. Gao,⁶ I. Garzia,^{24a,24b} P. T. Ge,⁶⁸ C. Geng,⁵⁰ E. M. Gersabeck,⁵⁸ K. Goetzen,¹¹ L. Gong,³³ W. X. Gong,^{1,49} W. Gradl,²⁸ M. Greco,^{66a,66c} L. M. Gu,³⁵ M. H. Gu,^{1,49} S. Gu,² Y. T. Gu,¹³ C. Y. Guan,^{1,54} A. Q. Guo,²² L. B. Guo,³⁴ R. P. Guo,⁴⁰ Y. P. Guo,^{9,h} A. Guskov,²⁹ T. T. Han,⁴¹ W. Y. Han,³² X. Q. Hao,¹⁶ F. A. Harris,⁵⁶ H. Hüskens,^{22,28} K. L. He,^{1,54} F. H. Heinsius,⁴ C. H. Heinz,²⁸ T. Held,⁴ Y. K. Heng,^{1,49,54} C. Herold,⁵¹ M. Himmelreich,^{11,f} T. Holtmann,⁴ Y. R. Hou,⁵⁴ Z. L. Hou,¹ H. M. Hu,^{1,54} J. F. Hu,^{47,m} T. Hu,^{1,49,54} Y. Hu,¹ G. S. Huang,^{63,49} L. Q. Huang,⁶⁴ X. T. Huang,⁴¹ Y. P. Huang,¹ Z. Huang,^{38,k} T. Hussain,⁶⁵ W. Ikegami Andersson,⁶⁷ W. Imoehl,²² M. Irshad,^{63,49} S. Jaeger,⁴ S. Janchiv,^{26,j} Q. Ji,¹ Q. P. Ji,¹⁶ X. B. Ji,^{1,54} X. L. Ji,^{1,49} H. B. Jiang,⁴¹ X. S. Jiang,^{1,49,54} J. B. Jiao,⁴¹ Z. Jiao,¹⁸ S. Jin,³⁵ Y. Jin,⁵⁷ T. Johansson,⁶⁷ N. Kalantar-Nayestanaki,⁵⁵ X. S. Kang,³³ R. Kappert,⁵⁵ M. Kavatsyuk,⁵⁵ B. C. Ke,^{43,1} I. K. Keshk,⁴ A. Khoukaz,⁶⁰ P. Kiese,²⁸ R. Kiuchi,¹ R. Kliemt,¹¹ L. Koch,³⁰ O. B. Kolcu,^{53a,e} B. Kopf,⁴ M. Kuemmel,⁴ M. Kuessner,⁴ A. Kupsc,⁶⁷ M. G. Kurth,^{1,54} W. Kühn,³⁰ J. J. Lane,⁵⁸ J. S. Lange,³⁰ P. Larin,¹⁵ A. Lavanaia,²¹ L. Lavezzi,^{66a,66c} Z. H. Lei,^{63,49} H. Leithoff,²⁸ M. Lellmann,²⁸ T. Lenz,²⁸ C. Li,³⁹ C. H. Li,³² Cheng Li,^{63,49} D. M. Li,⁷¹ F. Li,^{1,49} G. Li,¹ H. Li,⁴³ H. Li,^{63,49} H. B. Li,^{1,54} H. J. Li,^{9,h} J. L. Li,⁴¹ J. Q. Li,⁴ J. S. Li,⁵⁰ Ke Li,¹ L. K. Li,¹ Lei Li,³ P. R. Li,³¹ S. Y. Li,⁵² W. D. Li,^{1,54} W. G. Li,¹ X. H. Li,^{63,49} X. L. Li,⁴¹ Z. Y. Li,⁵⁰ H. Liang,^{63,49} H. Liang,^{1,54} H. Liang,²⁷ Y. F. Liang,⁴⁵ Y. T. Liang,²⁵ L. Z. Liao,^{1,54} J. Libby,²¹ C. X. Lin,⁵⁰ B. J. Liu,¹ C. X. Liu,¹ D. Liu,^{63,49} F. H. Liu,⁴⁴ Fang Liu,¹ Feng Liu,⁶ H. B. Liu,¹³ H. M. Liu,^{1,54} Huanhuan Liu,¹ Huihui Liu,¹⁷ J. B. Liu,^{63,49} J. L. Liu,⁶⁴ J. Y. Liu,^{1,54} K. Liu,¹ K. Y. Liu,³³ Ke Liu,⁶ L. Liu,^{63,49} M. H. Liu,^{9,h} P. L. Liu,¹

Q. Liu,⁵⁴ Q. Liu,⁶⁸ S. B. Liu,^{63,49} Shuai Liu,⁴⁶ T. Liu,^{1,54} W. M. Liu,^{63,49} X. Liu,³¹ Y. Liu,³¹ Y. B. Liu,³⁶ Z. A. Liu,^{1,49,54}
 Z. Q. Liu,⁴¹ X. C. Lou,^{1,49,54} F. X. Lu,¹⁶ F. X. Lu,⁵⁰ H. J. Lu,¹⁸ J. D. Lu,^{1,54} J. G. Lu,^{1,49} X. L. Lu,¹ Y. Lu,¹ Y. P. Lu,^{1,49}
 C. L. Luo,³⁴ M. X. Luo,⁷⁰ P. W. Luo,⁵⁰ T. Luo,^{9,h} X. L. Luo,^{1,49} S. Lusso,^{66c} X. R. Lyu,⁵⁴ F. C. Ma,³³ H. L. Ma,¹ L. L. Ma,⁴¹
 M. M. Ma,^{1,54} Q. M. Ma,¹ R. Q. Ma,^{1,54} R. T. Ma,⁵⁴ X. X. Ma,^{1,54} X. Y. Ma,^{1,49} F. E. Maas,¹⁵ M. Maggiora,^{66a,66c}
 S. Maldaner,⁴ S. Malde,⁶¹ Q. A. Malik,⁶⁵ A. Mangoni,^{23b} Y. J. Mao,^{38,k} Z. P. Mao,¹ S. Marcello,^{66a,66c} Z. X. Meng,⁵⁷
 J. G. Messchendorp,⁵⁵ G. Mezzadri,^{24a} T. J. Min,³⁵ R. E. Mitchell,²² X. H. Mo,^{1,49,54} Y. J. Mo,⁶ N. Yu. Muchnoi,^{10,c}
 H. Muramatsu,⁵⁹ S. Nakhoul,^{11,f} Y. Nefedov,²⁹ F. Nerling,^{11,f} I. B. Nikolaev,^{10,c} Z. Ning,^{1,49} S. Nisar,^{8,i} S. L. Olsen,⁵⁴
 Q. Ouyang,^{1,49,54} S. Pacetti,^{23b,23c} X. Pan,^{9,h} Y. Pan,⁵⁸ A. Pathak,¹ P. Patteri,^{23a} M. Pelizaeus,⁴ H. P. Peng,^{63,49} K. Peters,^{11,f}
 J. Pettersson,⁶⁷ J. L. Ping,³⁴ R. G. Ping,^{1,54} R. Poling,⁵⁹ V. Prasad,^{63,49} H. Qi,^{63,49} H. R. Qi,⁵² K. H. Qi,²⁵ M. Qi,³⁵ T. Y. Qi,⁹
 T. Y. Qi,² S. Qian,^{1,49} W.-B. Qian,⁵⁴ Z. Qian,⁵⁰ C. F. Qiao,⁵⁴ L. Q. Qin,¹² X. S. Qin,⁴ Z. H. Qin,^{1,49} J. F. Qiu,¹ S. Q. Qu,³⁶
 K. H. Rashid,⁶⁵ K. Ravindran,²¹ C. F. Redmer,²⁸ A. Rivetti,^{66c} V. Rodin,⁵⁵ M. Rolo,^{66c} G. Rong,^{1,54} Ch. Rosner,¹⁵
 M. Rump,⁶⁰ H. S. Sang,⁶³ A. Sarantsev,^{29,d} Y. Schelhaas,²⁸ C. Schmier,⁴ K. Schoenning,⁶⁷ M. Scodreggio,^{24a,24b} D. C. Shan,⁴⁶
 W. Shan,¹⁹ X. Y. Shan,^{63,49} J. F. Shangguan,⁴⁶ M. Shao,^{63,49} C. P. Shen,⁹ P. X. Shen,³⁶ X. Y. Shen,^{1,54} H. C. Shi,^{63,49}
 R. S. Shi,^{1,54} X. Shi,^{1,49} X. D. Shi,^{63,49} W. M. Song,^{27,1} Y. X. Song,^{38,k} S. Sosio,^{66a,66c} S. Spataro,^{66a,66c} K. X. Su,⁶⁸ P. P. Su,⁴⁶
 F. F. Sui,⁴¹ G. X. Sun,¹ H. K. Sun,¹ J. F. Sun,¹⁶ L. Sun,⁶⁸ S. S. Sun,^{1,54} T. Sun,^{1,54} W. Y. Sun,³⁴ W. Y. Sun,²⁷ X. Sun,^{20,1}
 Y. J. Sun,^{63,49} Y. K. Sun,^{63,49} Y. Z. Sun,¹ Z. T. Sun,¹ Y. H. Tan,⁶⁸ Y. X. Tan,^{63,49} C. J. Tang,⁴⁵ G. Y. Tang,¹ J. Tang,⁵⁰
 J. X. Teng,^{63,49} V. Thoren,⁶⁷ I. Uman,^{53b} B. Wang,¹ C. W. Wang,³⁵ D. Y. Wang,^{38,k} H. J. Wang,³¹ H. P. Wang,^{1,54} K. Wang,^{1,49}
 L. L. Wang,¹ M. Wang,⁴¹ M. Z. Wang,^{38,k} Meng Wang,^{1,54} W. Wang,⁵⁰ W. H. Wang,⁶⁸ W. P. Wang,^{63,49} X. Wang,^{38,k}
 X. F. Wang,³¹ X. L. Wang,^{9,h} Y. Wang,⁵⁰ Y. Wang,^{63,49} Y. D. Wang,³⁷ Y. F. Wang,^{1,49,54} Y. Q. Wang,¹ Y. Y. Wang,³¹
 Z. Wang,^{1,49} Z. Y. Wang,¹ Ziyi Wang,⁵⁴ Zongyuan Wang,^{1,54} D. H. Wei,¹² P. Weidenkaff,²⁸ F. Weidner,⁶⁰ S. P. Wen,¹
 D. J. White,⁵⁸ U. Wiedner,⁴ G. Wilkinson,⁶¹ M. Wolke,⁶⁷ L. Wollenberg,⁴ J. F. Wu,^{1,54} L. H. Wu,¹ L. J. Wu,^{1,54} X. Wu,^{9,h}
 Z. Wu,^{1,49} L. Xia,^{63,49} H. Xiao,^{9,h} S. Y. Xiao,¹ Z. J. Xiao,³⁴ X. H. Xie,^{38,k} Y. G. Xie,^{1,49} Y. H. Xie,⁶ T. Y. Xing,^{1,54} G. F. Xu,¹
 Q. J. Xu,¹⁴ W. Xu,^{1,54} X. P. Xu,⁴⁶ F. Yan,^{9,h} L. Yan,^{9,h} W. B. Yan,^{63,49} W. C. Yan,⁷¹ Xu Yan,⁴⁶ H. J. Yang,^{42,g} H. X. Yang,¹
 L. Yang,⁴³ S. L. Yang,⁵⁴ Y. X. Yang,¹² Yifan Yang,^{1,54} Zhi Yang,²⁵ M. Ye,^{1,49} M. H. Ye,⁷ J. H. Yin,¹ Z. Y. You,⁵⁰
 B. X. Yu,^{1,49,54} C. X. Yu,³⁶ G. Yu,^{1,54} J. S. Yu,^{20,1} T. Yu,⁶⁴ C. Z. Yuan,^{1,54} L. Yuan,² X. Q. Yuan,^{38,k} Y. Yuan,¹ Z. Y. Yuan,⁵⁰
 C. X. Yue,³² A. Yuncu,^{53a,a} A. A. Zafar,⁶⁵ Y. Zeng,^{20,1} B. X. Zhang,¹ Guangyi Zhang,¹⁶ H. Zhang,⁶³ H. H. Zhang,⁵⁰
 H. H. Zhang,²⁷ H. Y. Zhang,^{1,49} J. J. Zhang,⁴³ J. L. Zhang,⁶⁹ J. Q. Zhang,³⁴ J. W. Zhang,^{1,49,54} J. Y. Zhang,¹ J. Z. Zhang,^{1,54}
 Jianyu Zhang,^{1,54} Jiawei Zhang,^{1,54} L. Q. Zhang,⁵⁰ Lei Zhang,³⁵ S. Zhang,⁵⁰ S. F. Zhang,³⁵ Shulei Zhang,^{20,1} X. D. Zhang,³⁷
 X. Y. Zhang,⁴¹ Y. Zhang,⁶¹ Y. H. Zhang,^{1,49} Y. T. Zhang,^{63,49} Yan Zhang,^{63,49} Yao Zhang,¹ Yi Zhang,^{9,h} Z. H. Zhang,⁶
 Z. Y. Zhang,⁶⁸ G. Zhao,¹ J. Zhao,³² J. Y. Zhao,^{1,54} J. Z. Zhao,^{1,49} Lei Zhao,^{63,49} Ling Zhao,¹ M. G. Zhao,³⁶ Q. Zhao,¹
 S. J. Zhao,⁷¹ Y. B. Zhao,^{1,49} Y. X. Zhao,²⁵ Z. G. Zhao,^{63,49} A. Zhemchugov,^{29,b} B. Zheng,⁶⁴ J. P. Zheng,^{1,49} Y. Zheng,^{38,k}
 Y. H. Zheng,⁵⁴ B. Zhong,³⁴ C. Zhong,⁶⁴ L. P. Zhou,^{1,54} Q. Zhou,^{1,54} X. Zhou,⁶⁸ X. K. Zhou,⁵⁴ X. R. Zhou,^{63,49} A. N. Zhu,^{1,54}
 J. Zhu,³⁶ K. Zhu,¹ K. J. Zhu,^{1,49,54} S. H. Zhu,⁶² T. J. Zhu,⁶⁹ W. J. Zhu,^{9,h} W. J. Zhu,³⁶ Y. C. Zhu,^{63,49} Z. A. Zhu,^{1,54}
 B. S. Zou,¹ and J. H. Zou¹

(BESIII Collaboration)

¹*Institute of High Energy Physics, Beijing 100049, People's Republic of China*²*Beihang University, Beijing 100191, People's Republic of China*³*Beijing Institute of Petrochemical Technology, Beijing 102617, People's Republic of China*⁴*Bochum Ruhr-University, D-44780 Bochum, Germany*⁵*Carnegie Mellon University, Pittsburgh, Pennsylvania 15213, USA*⁶*Central China Normal University, Wuhan 430079, People's Republic of China*⁷*China Center of Advanced Science and Technology, Beijing 100190, People's Republic of China*⁸*COMSATS University Islamabad, Lahore Campus, Defence Road, Off Raiwind Road, 54000 Lahore, Pakistan*⁹*Fudan University, Shanghai 200443, People's Republic of China*¹⁰*G.I. Budker Institute of Nuclear Physics SB RAS (BINP), Novosibirsk 630090, Russia*¹¹*GSI Helmholtzcentre for Heavy Ion Research GmbH, D-64291 Darmstadt, Germany*¹²*Guangxi Normal University, Guilin 541004, People's Republic of China*¹³*Guangxi University, Nanning 530004, People's Republic of China*¹⁴*Hangzhou Normal University, Hangzhou 310036, People's Republic of China*

- ¹⁵*Helmholtz Institute Mainz, Johann-Joachim-Becher-Weg 45, D-55099 Mainz, Germany*
- ¹⁶*Henan Normal University, Xinxiang 453007, People's Republic of China*
- ¹⁷*Henan University of Science and Technology, Luoyang 471003, People's Republic of China*
- ¹⁸*Huangshan College, Huangshan 245000, People's Republic of China*
- ¹⁹*Hunan Normal University, Changsha 410081, People's Republic of China*
- ²⁰*Hunan University, Changsha 410082, People's Republic of China*
- ²¹*Indian Institute of Technology Madras, Chennai 600036, India*
- ²²*Indiana University, Bloomington, Indiana 47405, USA*
- ^{23a}*INFN Laboratori Nazionali di Frascati, I-00044, Frascati, Italy*
- ^{23b}*INFN Sezione di Perugia, I-06100, Perugia, Italy*
- ^{23c}*University of Perugia, I-06100, Perugia, Italy*
- ^{24a}*INFN Sezione di Ferrara, I-44122, Ferrara, Italy*
- ^{24b}*University of Ferrara, I-44122, Ferrara, Italy*
- ²⁵*Institute of Modern Physics, Lanzhou 730000, People's Republic of China*
- ²⁶*Institute of Physics and Technology, Peace Ave. 54B, Ulaanbaatar 13330, Mongolia*
- ²⁷*Jilin University, Changchun 130012, People's Republic of China*
- ²⁸*Johannes Gutenberg University of Mainz, Johann-Joachim-Becher-Weg 45, D-55099 Mainz, Germany*
- ²⁹*Joint Institute for Nuclear Research, 141980 Dubna, Moscow region, Russia*
- ³⁰*Justus-Liebig-Universitaet Giessen, II. Physikalisches Institut, Heinrich-Buff-Ring 16, D-35392 Giessen, Germany*
- ³¹*Lanzhou University, Lanzhou 730000, People's Republic of China*
- ³²*Liaoning Normal University, Dalian 116029, People's Republic of China*
- ³³*Liaoning University, Shenyang 110036, People's Republic of China*
- ³⁴*Nanjing Normal University, Nanjing 210023, People's Republic of China*
- ³⁵*Nanjing University, Nanjing 210093, People's Republic of China*
- ³⁶*Nankai University, Tianjin 300071, People's Republic of China*
- ³⁷*North China Electric Power University, Beijing 102206, People's Republic of China*
- ³⁸*Peking University, Beijing 100871, People's Republic of China*
- ³⁹*Qufu Normal University, Qufu 273165, People's Republic of China*
- ⁴⁰*Shandong Normal University, Jinan 250014, People's Republic of China*
- ⁴¹*Shandong University, Jinan 250100, People's Republic of China*
- ⁴²*Shanghai Jiao Tong University, Shanghai 200240, People's Republic of China*
- ⁴³*Shanxi Normal University, Linfen 041004, People's Republic of China*
- ⁴⁴*Shanxi University, Taiyuan 030006, People's Republic of China*
- ⁴⁵*Sichuan University, Chengdu 610064, People's Republic of China*
- ⁴⁶*Soochow University, Suzhou 215006, People's Republic of China*
- ⁴⁷*South China Normal University, Guangzhou 510006, People's Republic of China*
- ⁴⁸*Southeast University, Nanjing 211100, People's Republic of China*
- ⁴⁹*State Key Laboratory of Particle Detection and Electronics, Beijing 100049, Hefei 230026, People's Republic of China*
- ⁵⁰*Sun Yat-Sen University, Guangzhou 510275, People's Republic of China*
- ⁵¹*Suranaree University of Technology, University Avenue 111, Nakhon Ratchasima 30000, Thailand*
- ⁵²*Tsinghua University, Beijing 100084, People's Republic of China*
- ^{53a}*Turkish Accelerator Center Particle Factory Group, Istanbul Bilgi University, 34060 Eyup, Istanbul, Turkey*
- ^{53b}*Near East University, Nicosia, North Cyprus, Mersin 10, Turkey*
- ⁵⁴*University of Chinese Academy of Sciences, Beijing 100049, People's Republic of China*
- ⁵⁵*University of Groningen, NL-9747 AA Groningen, The Netherlands*
- ⁵⁶*University of Hawaii, Honolulu, Hawaii 96822, USA*
- ⁵⁷*University of Jinan, Jinan 250022, People's Republic of China*
- ⁵⁸*University of Manchester, Oxford Road, Manchester, M13 9PL, United Kingdom*
- ⁵⁹*University of Minnesota, Minneapolis, Minnesota 55455, USA*
- ⁶⁰*University of Muenster, Wilhelm-Klemm-Str. 9, 48149 Muenster, Germany*
- ⁶¹*University of Oxford, Keble Rd, Oxford, UK OX13RH*
- ⁶²*University of Science and Technology Liaoning, Anshan 114051, People's Republic of China*
- ⁶³*University of Science and Technology of China, Hefei 230026, People's Republic of China*
- ⁶⁴*University of South China, Hengyang 421001, People's Republic of China*
- ⁶⁵*University of the Punjab, Lahore-54590, Pakistan*
- ^{66a}*University of Turin and INFN, University of Turin, I-10125, Turin, Italy*
- ^{66b}*University of Eastern Piedmont, I-15121, Alessandria, Italy*

^{66c}*INFN, I-10125, Turin, Italy*⁶⁷*Uppsala University, Box 516, SE-75120 Uppsala, Sweden*⁶⁸*Wuhan University, Wuhan 430072, People's Republic of China*⁶⁹*Xinyang Normal University, Xinyang 464000, People's Republic of China*⁷⁰*Zhejiang University, Hangzhou 310027, People's Republic of China*⁷¹*Zhengzhou University, Zhengzhou 450001, People's Republic of China*⁷²*Yunnan University, Kunming 650500, People's Republic of China*^aAlso at Bogazici University, 34342 Istanbul, Turkey.^bAlso at the Moscow Institute of Physics and Technology, Moscow 141700, Russia.^cAlso at the Novosibirsk State University, Novosibirsk, 630090, Russia.^dAlso at the NRC "Kurchatov Institute", PNPI, 188300, Gatchina, Russia.^eAlso at Istanbul Arel University, 34295 Istanbul, Turkey.^fAlso at Goethe University Frankfurt, 60323 Frankfurt am Main, Germany.^gAlso at Key Laboratory for Particle Physics, Astrophysics and Cosmology, Ministry of Education; Shanghai Key Laboratory for Particle Physics and Cosmology; Institute of Nuclear and Particle Physics, Shanghai 200240, People's Republic of China.^hAlso at Key Laboratory of Nuclear Physics and Ion-beam Application (MOE) and Institute of Modern Physics, Fudan University, Shanghai 200443, People's Republic of China.ⁱAlso at Harvard University, Department of Physics, Cambridge, MA, 02138, USA.^jCurrently at: Institute of Physics and Technology, Peace Ave.54B, Ulaanbaatar 13330, Mongolia.^kAlso at State Key Laboratory of Nuclear Physics and Technology, Peking University, Beijing 100871, People's Republic of China.^lSchool of Physics and Electronics, Hunan University, Changsha 410082, China.^mAlso at Guangdong Provincial Key Laboratory of Nuclear Science, Institute of Quantum Matter, South China Normal University, Guangzhou 510006, China.